

PAPER • OPEN ACCESS

## Electromagnetic interference filter for spacecraft power bus

To cite this article: Y S Zhechev *et al* 2019 *IOP Conf. Ser.: Mater. Sci. Eng.* **560** 012133

View the [article online](#) for updates and enhancements.



**IOP | ebooks™**

Bringing you innovative digital publishing with leading voices to create your essential collection of books in STEM research.

Start exploring the [collection](#) - download the first chapter of every title for free.

# Electromagnetic interference filter for spacecraft power bus

Y S Zhechev, V P Kosteletskii, A M Zabolotsky and T R Gazizov

Scientific Research Laboratory of Safety Electromagnetic Compatibility of Radioelectronics Equipment, Tomsk State University of Control Systems and Radioelectronics, 40 Lenin Avenue, Tomsk 634050, Russian Federation

E-mail: [geopath@mail.ru](mailto:geopath@mail.ru)

**Abstract.** The paper considers the protection of radio-electronic equipment against common and differential mode interference by means of a filter based on lumped elements. The authors have developed a schematic diagram of the filter to be used in power supply circuits of a spacecraft, and present and compare the results of circuit simulation and experiment. The results are useful for further development of noise protection devices for the spacecraft power bus.

## 1. Introduction

Currently, the importance of ensuring noise immunity of industrial radioelectronic equipment (REE), including the onboard REE of a spacecraft, is increasing. Sources of secondary power supply expand the range of operating frequencies to increase the efficiency of conversion. This fact adversely affects the electromagnetic environment. Conducted and radiated interferences are generated by the processes of switching power switches of the converters [1]. Conducted interferences represent the greatest danger to REE due to the spectral width and impact power [2]. The power bus is an important element of the spacecraft electric power supply system, therefore its noise immunity is important [3].

Interference filters are used to limit the conducted interference level. Electromagnetic interference (EMI) filters are characterized by the frequency dependence of the insertion losses. There are special requirements to the spacecraft EMI filters, including increased reliability, radiation resistance, service life of 15 – 20 years and lowest weight-size parameters [4,5]. However, there are few publications on complete designs of passive EMI filters for spacecrafts. The aim of this paper is to fill this gap.

## 2. Approaches, schematic diagram and structure

The basis of the device under development is a low-pass filter on lumped elements, which has a third-order Butterworth characteristic. These filtering devices have the flattest amplitude-frequency characteristic (AFC) in the passband. The gain slope meets technical requirements and is 60 dB/dec for common and differential modes. In contrast to other protection devices, there are no active components in the developed filter [6–8]. As a result, the device fully conforms to [9] and has the required reliability. To check circuit integrity and conduct analysis in the time and frequency domains, we used SPICE simulation. It allows providing necessary technical characteristics of the developed device at minimal time and economic costs.

SPICE simulation is successfully used to simulate electronic circuits and components, and is based on the analysis of a circuit using the nodal potential method, which is necessary to derive the equations of the total circuit. Complex SPICE models are based on passive R, L, C components, as well as



current and voltage sources [10]. The study used this method.

The EMI filter (figure 1) includes a common mode choke with the highest inductance for common mode interference, 2 uncoupled chokes to attenuate differential interference, and 4 ceramic capacitors. Two damping resistors can attenuate high frequency emissions and reduce unwanted reactive currents. However, the resistors are shorted in this study.

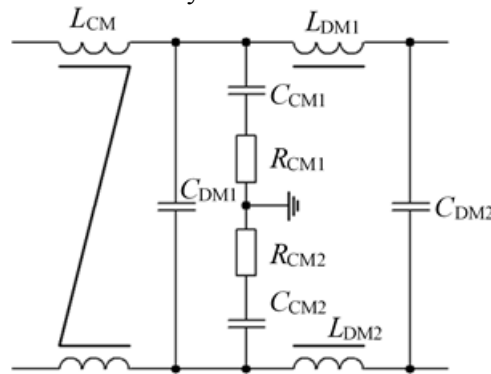


**Figure 1.** Schematic diagram of the developed filter.

The selected diagram, in the absence of EMI, hardly ever affects the operation of the protected circuit, has a necessary response to a high rate of current and voltage rise as well as a required current capacity [11]. We developed a schematic simulation model based on expressions from [12]. The developed EMI filter (Figure 1) is based on 2 functional circuit models for suppressing the differential and common modes of EMI (Figure 2).

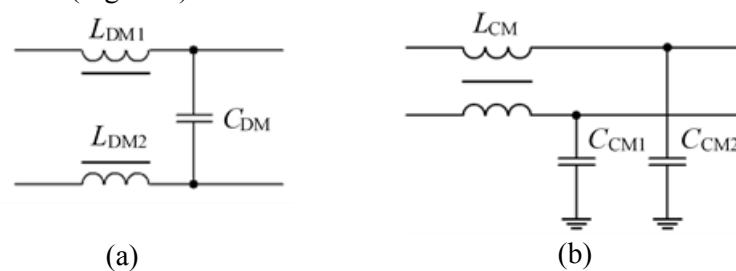


**Figure 2.** Functional circuit models for suppressing the differential (a) and common (b) modes of EMI.

To suppress the differential mode of EMI, we used 2 series-connected chokes  $L_{DM1}$ ,  $L_{DM2}$  and 2 parallel-connected capacitors  $C_{DM1}$ ,  $C_{DM2}$ . Expressions for calculating component values [12] are:

$$C_{DM} = \frac{1}{2\pi f_{DM} R_f}, \quad L_{DM} = \frac{R_f}{2\pi f_{DM}} \quad (1)$$

where  $C_{DM}$  is capacitance of the differential capacitor,  $L_{DM}$  is inductance of the differential choke,  $R_f$  is output impedance of the filter, and  $f_{DM}$  is cutoff frequency of the filter for the differential mode (by the level of -3 dB).

To suppress the EMI common-mode, the common-mode choke of the  $L_{CM}$  and 2 capacitors  $C_{CM1}$ ,  $C_{CM2}$  are used, which shunt each line to the ground conductor. To calculate the values of the components, we used following expressions [12]:

$$f_{CM} = \frac{1}{2\pi\sqrt{L_{CM}C_{CM}}}, \quad C_{CM} = \frac{1}{(2\pi)^2 f_{CM}^2 L_{CM}} \quad (2)$$

where  $C_{CM}$  is capacitance of the common-mode capacitor,  $L_{CM}$  is inductance of the common-mode choke,  $f_{CM}$  is cut-off frequency of the filter for the common mode EMI (by the level of -3 dB).

To achieve the required inductance of chokes, we determined the number of turns and the core material which defines the operating temperature, frequency and high-frequency losses. To calculate the required number of turns of the defined wire cross section, the following expression was used [13]:

$$L = 0.0002 \mu h N^2 \ln \frac{D_1}{D_2} \quad (3)$$

where  $h$  is the height of the ferrite ring;  $D_1$  and  $D_2$  are the outer and inner diameters of the ring respectively;  $N$  is the number of turns;  $\mu$  is the magnetic permeability of the core.

### 3. Results and discussion

The nominal values of the EMI filter components were calculated on the basis of the following technical characteristics:  $f_{CM} = 37$  kHz,  $f_{DM} = 9$  kHz,  $R_f = 50 \Omega$ . The simulation was carried out taking into account parasitic parameters of the components, the equivalent circuits of which are depicted in Figure 3.

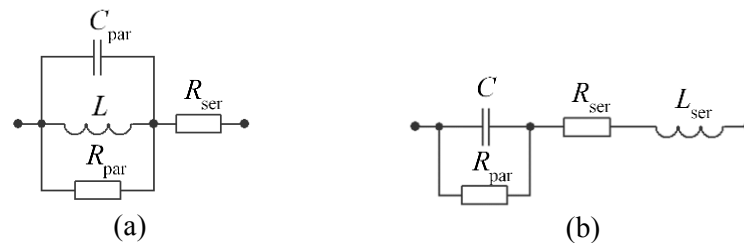


**Figure 3.** Equivalent circuits of a choke (a) and a capacitor (b).

To implement the differential choke, we used a PETV2 wire with a diameter of 0.28 mm and a ferrite core MP140-6 with the following geometrical parameters:  $D_1 = 13$  mm,  $D_2 = 7$  mm and  $h = 5$  mm. The inductance of the  $L_{DM}$  calculated by (1) is equal to 1049  $\mu$ H. The values of the measured parasitic parameters were  $R_{par} = 10$  M $\Omega$ ,  $R_{ser} = 0.5 \Omega$ ,  $C_{par} = 2.2$  nF. To realize the common-mode choke, we used a ferrite core of M250HMC7-58 type with geometric parameters:  $D_1 = 7$  mm,  $D_2 = 4$  mm,  $h = 2$  mm. To get the necessary current carrying capacity, a bifilar winding with a PETV2 wire of 0.2 mm diameter was used. The inductance  $L_{DM}$ , calculated according to (2), is equal to 126  $\mu$ H. The values of the measured parasitic parameters were:  $R_{par} = 10$  M $\Omega$ ,  $R_{ser} = 0.053 \Omega$ ,  $C_{par} = 0.3$  nF. By (3) we calculated the number of turns, which is 110 for the differential and 15 for the common-mode chokes. The differential capacitance  $C_{DM}$  was represented by the ceramic capacitor GRM43QR72J683KW01L with capacity of 66 nF. The values of the measured parasitic parameters of the capacitor were  $R_{par} = 10$  M $\Omega$ ,  $R_{ser} = 0.02 \Omega$ ,  $L_{ser} = 10$  nH. A ceramic capacitor 2225GC333KAT1A with a capacity of 33 nF was chosen to implement the common-mode capacitance  $C_{CM}$ . The values of the measured parasitic parameters of  $C_{CM}$  were  $R_{par} = 10$  M $\Omega$ ,  $R_{ser} = 0.015 \Omega$ ,  $L_{ser} = 15$  nH. The parasitic parameters were obtained using the Rohde & Schwarz HM8118 immittance meter. The schematic diagrams for conducting circuit simulation in the common and differential modes are presented in Figure 4. For common-mode simulation, both filter inputs are connected to a generator and both outputs are connected to the load of the measuring path  $R_1 = 50 \Omega$ . In differential mode, the generator is connected between the input terminals of the filter, and the measurement is performed between the output terminals on the load  $R_2 = 100 \Omega$ . On the circuit models, the resistance of the U1 generator is not depicted; however, it is taken into account in the simulation and has the value of 50  $\Omega$ .

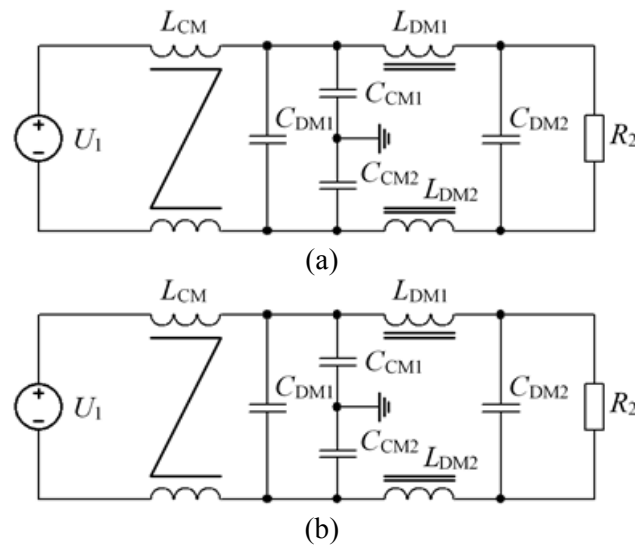


**Figure 4.** Circuit models of the filter for common (a) and differential (b) modes.

We have also developed the EMI filter prototype (Figure 5). The printed circuit board (PCB) of the filter was made with double redundancy of interconnections, in accordance with technical specifications for the development. The conductive parts of the filter are designed for direct current of 2 A with a double reserve margin.

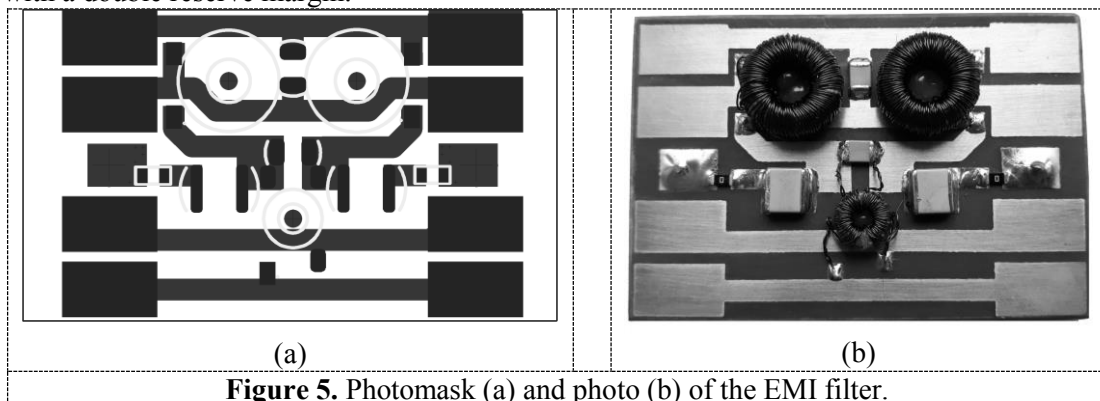


**Figure 5.** Photomask (a) and photo (b) of the EMI filter.

The results of the simulation and the experiment with the frequency of up to 1 GHz are presented in Figure 6 and Table 1. The deviation of the cut-off frequencies obtained using the circuit simulation and the experiment was 23.8% for the common and 38.46% for the differential modes. The forms of AFC in the simulation and the experiment for the common mode has a similar character. In the differential mode in the experimental data there is a resonance at frequency of 2 MHz. The difference in the frequency response in the simulation and the experiment for both modes is due to the peculiarities of the used mathematical apparatus and unaccounted parasitic parameters.

**Table 1.** Comparison of calculated and measured cut-off frequencies [kHz] for common and differential modes

Mode	Simulation	Experiment	Deviation, [%]
Common	40	65	23.81
Differential	4	9	38.46

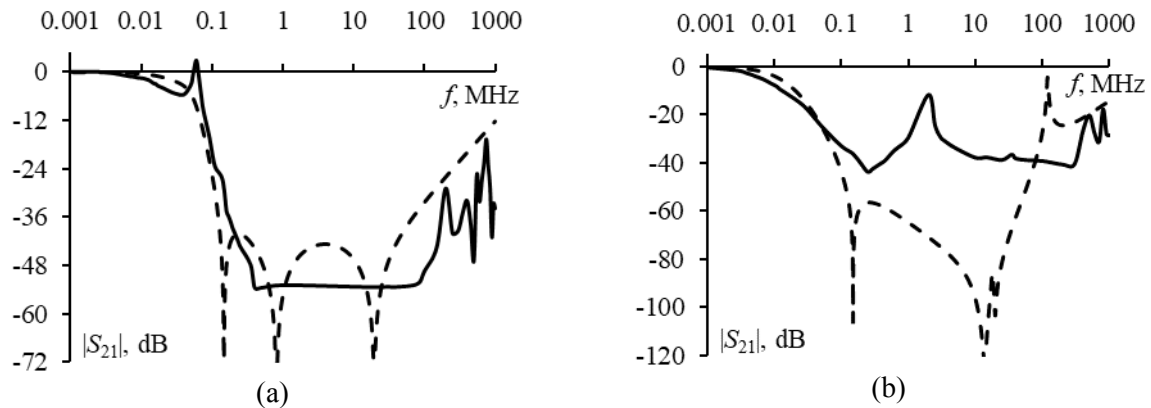


**Figure 6.** Comparison of experimental (—) and simulation (- -) results for common (a) and differential (b) modes.

#### 4. Conclusion

Thus, the study has presented the EMI filter based on lumped elements for the spacecraft power bus. In addition, we built a working prototype of the EMI filter. The comparison of the circuit simulation and experiment results revealed that the circuit simulation model allows designing a device for EMI protection with minimal computational effort. However, to obtain a reasonable consistency of simulation and experiment results, many parasitic parameters and mutual influence of circuit elements and PCB must be taken into account. Electrodynamics analysis is undoubtedly useful for this aim. Our future research will be dedicated to this detailed simulation.

#### Acknowledgment

The study was supported by the Ministry of Science and Higher Education of the Russian Federation (project RFMEFI57417 X0172).

#### References

- [1] Lehr J and Pralhad R 2017 *Foundations of Pulsed Power Technology* (New York: Wiley-IEEE Press) p 664
- [2] Gizatullin Z and Gizatullin R 2016 Investigation of the immunity of computer equipment to the power-line electromagnetic interference *J. of Communic. Technol. and Electron.* **5** 546–550
- [3] Iljin A and Semkin N 2015 *Registration of interference induced by the power bus 27V on board the spacecraft* (Samara: SSAU) pp 19–20
- [4] GOST R 56515-2015 *Automatic spacecrafts and onboard support spacecraft systems. General requirements for protection and resistance to electrophysical space factors and static electricity* 2016 (Standartinform, Moscow)
- [5] MIL-STD-1541A *Electromagnetic Compatibility Requirements for Space Systems* 1987 (USAF) p 42
- [6] Zhihong Y, Boroyevich D, Kun Xing, Lee F and Changrong Liu 1999 Active common-mode filter for inverter power supplies with unbalanced and nonlinear load *IEEE Industry Applications Conf.* **4** 1858–1864
- [7] Ping Wang, Chenbin Tao and Jinghai Zhang 2009 Research and design of a common mode hybrid EMI filter for switch-mode power supply *3rd Int. Conf. on Power Electron. Systems and Applicat.* p 4
- [8] Naoto Kikuchi and Tomohisa Hirono 2016 The active EMI filter for suppressing common-mode noise in bridge-less PFC converter system *19th Int. Conf. on Electrical Machines and Systems* p 6
- [9] GOST R 56529-2015 *Electromagnetic compatibility of space technology. General requirements*

- and test methods* 2016 (Standartinform, Moscow) p 64
- [10] Rewieński M 2011 *Simulation and Verification of Electronic and Biological Systems* (Springer) pp 23–42
- [11] Balyuk N, Boldyrev V and Bulekov V 2004 *Electromagnetic compatibility of technical equipment of movable facility* (Moscow: MAI) p 648
- [12] Richard L and Timothy M 2012 *EMI filter design* (CRC Press) p 264
- [13] Kalantarov P and Tseitlin L 1986 *Inductance calculation* (Energoatomizdat) p 481